

# Particle Size Influence Upon Sintered Induced Strains Within 3DP™ Stainless Steel Components

Scott Johnston,<sup>1,2</sup> Rhonda Anderson<sup>1,2</sup> and Duane Storti<sup>1,\*</sup>

<sup>1</sup> Dept. of Mechanical Engineering, University of Washington, Seattle, WA 98195-2600

<sup>2</sup> Concurrent Technologies Corporation, Bremerton, WA 98312

\*Author to whom correspondence should be addressed.

Reviewed, accepted August 19, 2003

## Abstract

Three-dimensional printing (3DP™<sup>1</sup>) is a layer-by-layer manufacturing process whereby a three-dimensional (3D) component is created by the distribution of a liquid binder onto a powder media. A 3DP™ process using stainless steel powder as its printing media requires post-printing thermal processing for debinding and sintering of the printed green component. To minimize dimensional distortion while increasing structural integrity of the green component, 3DP™ thermal post-processing is designed to produce only neck growth between particles, defined as initial stage sintering.

The accepted theoretical model governing initial stage sintering strain for spherical powder particles provides a qualitative account of strain development with respect to time and temperature variance; however, the model does not produce an accurate quantitative account for the magnitude of the strain when compared to dimensional experimental results. The theoretical model indicates that powder particle size is the dominant parameter governing sintering strain.

The purpose of this study is to introduce an effective particle size into the theoretical model, thus enabling the application of the theoretical model to estimate dimensional change for components produced by 3DP™. Dimensional sintering experimentation has been performed using 3DP™ test specimens with spherical powder particles having mean diameters of 20  $\mu\text{m}$ , 80  $\mu\text{m}$ , and 200  $\mu\text{m}$ . Experimental results and progress on the theoretical model are discussed.

## Introduction

It is extremely difficult to accurately predict the effects of sintering for dimensional, structural, and compositional changes due to the phenomenological aspects involved in sintering. Modeling efforts often result in inadequate approximations or inconclusive results. These approximations can be attributed to inaccurate material properties at sintering temperatures and non-rigorous understanding of basic relationships [1]. Most analytical sintering models provide qualitative illustrations of dimensional change (strain), but cannot quantitatively represent the magnitudes of these strains when applied to 3DP™ sintering process.

The widely accepted analytical formulation of initial stage sintering exhibiting an appropriate development of strain has been presented by German [2,3]. These equations are valid for isothermal conditions and provide a solid foundation for analysis of strain development of

---

<sup>1</sup> 3DP is a registered trademark of the Massachusetts Institute of Technology.

components manufactured by 3DP™. An expansion of these equations to allow for non-isothermal conditions is required in order to quantify some of the phenomenological aspects of initial stage sintering theory when applied to 3DP™ sintering practices.

This study emphasizes the analysis of strains produced from sintering stainless steel 3DP™ components. 3DP™ components are manufactured in a layer-by-layer construction using liquid binder applied to powdered materials [4]. This study is limited to analysis of components comprising a polymeric binder and 316L stainless steel (316L SS) powder with individual test specimens consisting of distinctively different particle diameters.

### Initial Stage Sintering Mechanisms

Sintering occurs in three stages: initial, intermediate, and final. In the 3DP™ process, sintering involves only initial stage sintering, which can be characterized by neck formation between adjacent particles [2,3], as illustrated in Figure 1. Neck formation can be reduced to surface transport mechanisms and bulk transport mechanisms; both of these contribute to the mass deposited within the neck. Only bulk mechanisms produce any shrinkage between particles, thereby producing strain. This analysis is concentrated solely on dimensional changes, so only bulk mechanisms are considered.

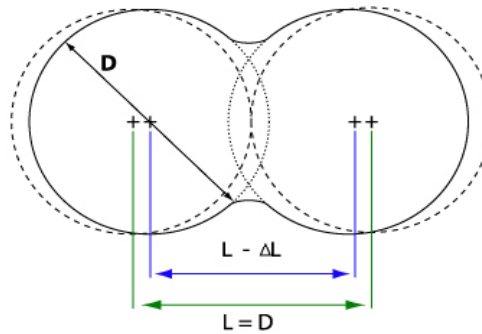


**Figure 1.** Dimensional representation of sintering neck growth and strain of two ideal spherical powder particles.

Initial stage sintering bulk mechanisms are comprised of plastic flow (PF), grain boundary diffusion (GB), and volume diffusion (VD) [2,3]. These three mechanisms affect the overall shrinkage of powder particles occurring from sintering. The relation of the associated parameters and their effective sintering strain, as produced between two spherical particles for each mechanism follows the basic kinetic law:

$$\left(\frac{\Delta L}{L}\right)^{n/2} = \varepsilon(t)^{n/2} = \frac{B \cdot t}{2^n D^m} \quad (1)$$

where  $t$  is time,  $D$  is the powder particle diameter, and  $L$  is the original length between the centers of the spherical particles (i.e., particle diameter).

Each mechanism is dependent on different material and physical parameters. The constant  $B$  depends on the specific sintering mechanism being considered and is exponentially related to temperature by the relationship:

$$B = B_o \exp\left(-\frac{Q_{mech}}{kT}\right) \quad (2)$$

where  $Q_{mech}$  is the activation energy for the corresponding mechanism, and the variables  $B_o$ ,  $m$ , and  $n$  are defined in Table 1.

**Table 1.** Summary of initial-stage sintering equations and parameters for spheres [2,3].

| Mechanism                       | $n$ | $m$                                | $B_o$                                  |
|---------------------------------|-----|------------------------------------|--|
| Volume diffusion (VD)           | 5   | 3                                  | $\frac{80\gamma D_v \Omega}{kT}$       |
| Grain boundary diffusion (GB)   | 6   | 4                                  | $\frac{20\delta\gamma D_b \Omega}{kT}$ |
| Plastic flow (PF)               | 2   | 1                                  | $\frac{9\pi\gamma b D_v}{kT}$          |
| <b>Symbols</b>                  |     |                                    |  |
| $\gamma$ = surface energy       |     | $D_v$ = volume diffusivity         |  |
| $\delta$ = grain boundary width |     | $D_b$ = grain boundary diffusivity |  |
| $\Omega$ = atomic volume        |     | $b$ = Burgers vector               |  |
| $k$ = Boltzmann's constant      |     | $T$ = Absolute temperature         |  |

The total strain produced is the superposition of all three bulk mechanisms, VD, GB, and PF. The bulk mechanisms will be the analytical basis used for a predictive analysis of sintering strains produced in 3DP™ components. An illustration of the qualitative strain development for VD is shown in Figure 2.

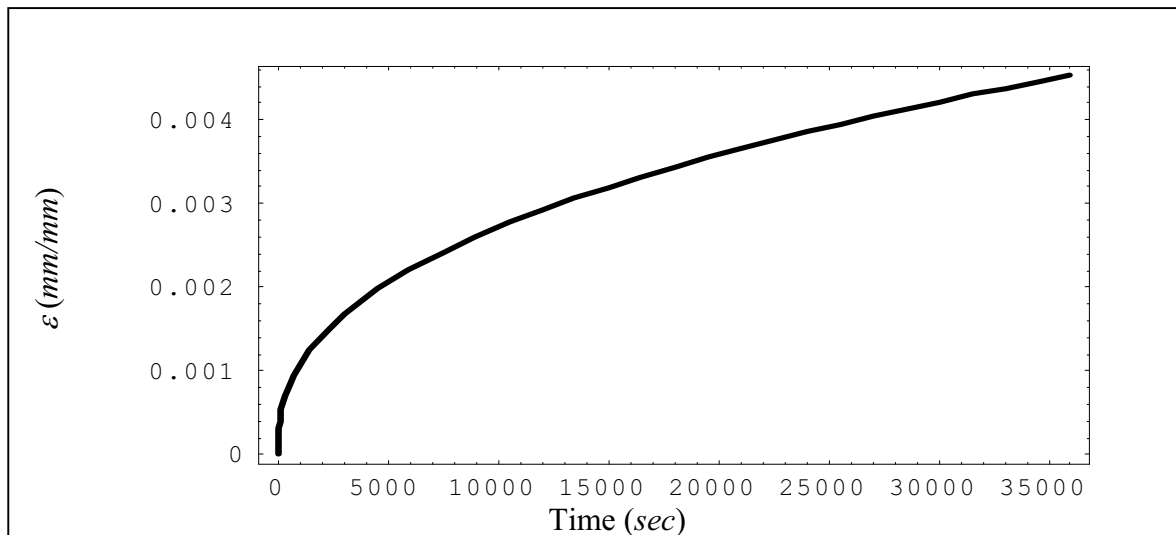


**Figure 2.** Isothermal sintering strain rate development for volume diffusion (VD) at 1500K for 10 hours.

The bulk mechanism equations presented in Equation 1 are valid for isothermal conditions; therefore, additional computational work must be developed in order to apply these equations to actual sintering temperature profiles. Hence, Equation 1 is more accurately represented as:

$$\varepsilon(t)_T = \left( \frac{B \cdot t}{2^n D^m} \right)^{2/n} \quad (1')$$

As mentioned previously, the total strain is the sum of the bulk mechanisms, VD, GB, and PF; since each mechanism depends upon different material properties, their contribution to the total strain is unequal. Volume diffusion has been identified as the dominating bulk mechanism by Thümmeler [5]. It can be observed from Table 2 that the strain produced from VD is the dominating bulk mechanism, while GB diffusion contributes less than 0.01% of the total strain, and PF's contribution is negligible. Therefore, only VD will be considered during strain calculations for this analysis.

**Table 2.** Strain values for 316L SS bulk mechanisms with varying particle diameter, isothermal temperature of 1500K, and 10-hour sintering time.

| Powder Particle Diameter ( $\mu m$ ) | Strain due to Volume Diffusion | Strain due to Plastic Flow | Strain due to Grain Boundary Diffusion |
|--------------------------------------|--------------------------------|----------------------------|--|
| 20                                   | 0.02393                        | $2.528 \times 10^{-20}$    | $2.248 \times 10^{-5}$                 |
| 80                                   | 0.00453                        | $6.319 \times 10^{-21}$    | $3.540 \times 10^{-6}$                 |
| 200                                  | 0.00151                        | $2.528 \times 10^{-21}$    | $1.043 \times 10^{-6}$                 |

### Analytical Calculation of Strain

Equation 1' represents initial stage sintering strain formulation under isothermal conditions. Consequently, Equation 1' is only valid once a temperature has been selected. This is an idealistic model because it assumes that a component instantly achieves a sintering temperature; but, for practical applications, a component begins at room temperature and heat is applied until a desired sintering temperature is reached. As a result, the component is traversing through a series of isothermal strain curves described by Equation 1'. Once a desired temperature is constantly sustained, then strain can be computed by the isothermal strain curve represented by Equation 1'.

Strain is not only produced at the sintering temperature, but at temperatures below the sintering temperature [6]. Strain has already started to form before the maximum temperature of the thermal cycle is reached and the calculation of strain must consider the current level of strain as well as the current temperature. Since a 3DP™ sintering profile involves a temperature decrease as well as increase (i.e., the component must be cooled in order to be handled), knowledge of whether the temperature is increasing or decreasing is essential. The reason for incorporating a relationship between previously produced strain and the corresponding temperature gradient allows for correct transition between higher and lower level isothermal strain curves, thereby including any additional strain that may be produced prior to and after reaching the desired sintering temperature.

### Strain rate surface, $\dot{\varepsilon}(t)_T$ ,

In order to perform a calculation of strain produced from a sintering temperature profile using isothermal strain curves required the introduction of a strain rate surface. It can be observed from Figure 2 that amount of strain produced at any time is dependant upon the temperature and the current level of strain. Namely, strain increases at greater rates at the beginning of isothermal time-strain curves produced from Equation 1'. It is reasonable to postulate that sintering strain can be calculated by summing the area under a strain rate surface over a defined temperature profile.

The creation of a strain rate surface that is dependant upon strain level and temperature is formulated using Equation 1' and *Mathematica* [7]. The premise is to choose specified strain increments and temperature increments that span the range of the temperature profile,  $T_{profile}(t)$ . The strain rates are then algebraically calculated at each of these strains and temperatures using Equation 1'.

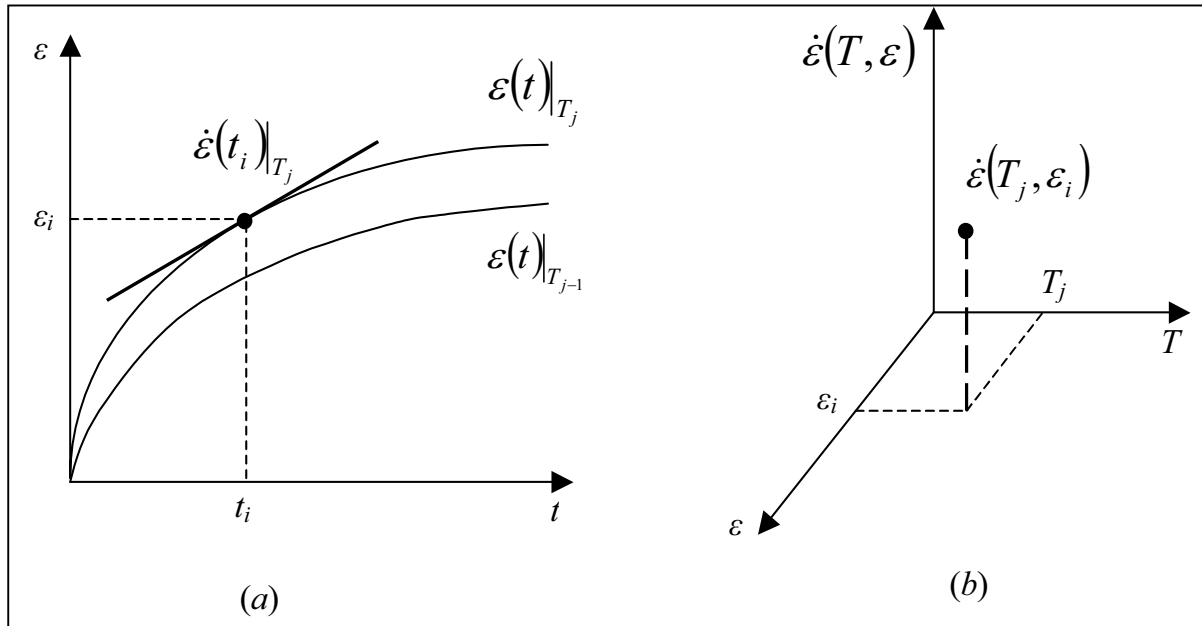


**Figure 3.** Graphical representation of construction of strain rate surface,  $\dot{\varepsilon}(t, T)$ ; (a) strain development for a mechanism, (b) strain rate plotted according to value of strain and time.

To create the strain rate surface, the temperature domain is divided into  $n$  discrete temperatures  $T_j$ . Since temperature has an important role in sintering activity, a coarse  $\Delta T$  is used at lower temperatures where the sintering activity is almost non-existent, and a finer  $\Delta T$  is used at elevated temperatures where sintering activity is high. The primary reason for performing this varied  $\Delta T$  is to reduce computation time. To ensure that the strain rate surface will contain every possible strain-temperature combination for the defined temperature profile, the maximum strain is computed at a temperature that exceeds the highest temperature achieved in the profile for a time period equal to the length of the profile.

One difficulty in creating the strain rate surface,  $\dot{\varepsilon}(t_i)|_{T_j}$ , involves how strain is defined. Strain is dependent upon time,  $t$ , and defined in terms of temperature,  $T$ . For each  $\varepsilon_i$  and  $T_j$  it is necessary to find an associated time,  $t_{ij}$ , where  $t_{ij} \equiv$  time required to reach strain  $\varepsilon_i$  at temperature,  $T_j$ . Finally, the strain rate may be calculated using Equation 3, and is represented graphically in Figure 3.

$$\dot{\varepsilon}(t_i)|_{T_j} = \dot{\varepsilon}(t_{ij}) = \dot{\varepsilon}(T_j, \varepsilon_i) \quad (3)$$

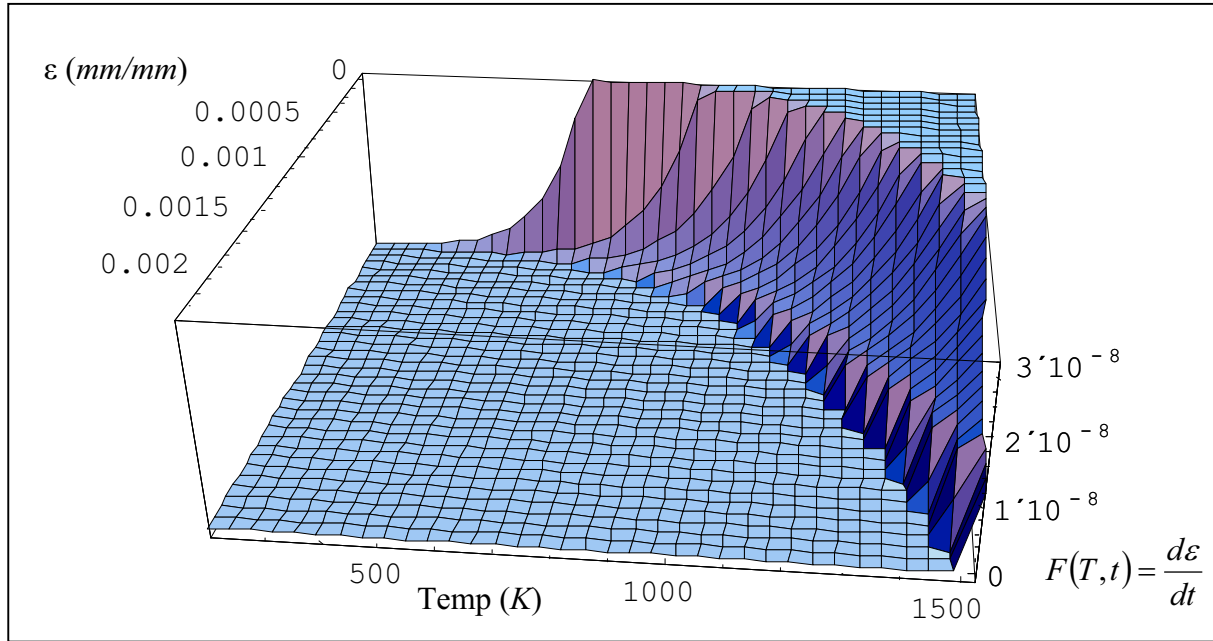


**Figure 4.** Strain rate surface for volume diffusion (VD).

The resulting strain rate surface (Figure 4) illustrates that at small values of existing strain, the strain rate is large and increases as the temperature increases, whereas at large values of current strain, the sintering strain rate is negligible. Both of these behaviors correspond to defining the strain rate as the tangential value to the curve shown in Figure 2.

#### Strain calculation using strain rate surface, $\dot{\varepsilon}(t_i)|_{T_j}$ for a defined temperature profile

The goal of creating the strain rate surface is to predict dimensional changes occurring during initial stage sintering of 3DP™ components using a defined temperature profile. Calculating the strain involves solving an ordinary differential equation (ODE) that incorporates the temperature profile. Representing the strain rate surface as  $F(T, \varepsilon)$ , it is possible to solve for a time-strain curve that is the result of a specified temperature profile,  $T_{profile}$ . A formal mathematical expression of this expression can be written as:

$$\frac{d\varepsilon}{dt} = F(T_{profile}(t), \varepsilon(t)) \quad (4)$$

where  $\varepsilon(t)$  is the strain at the corresponding time and temperature of  $T_{profile}$  (defined by Equation 1') and the initial condition  $\varepsilon(0) = 0$ . The solution to this ODE is a time-strain curve representing the amount of strain (shrinkage) produced between two equally sized spherical powder particles.

### Experimental Results Compared to Analytical Calculations

To validate the analytical formulation presented herein, theoretical results were compared to experimental measurements using 316L SS samples. Components were manufactured on a ProMetal RTS-300, a solid freeform fabrication machine capable of creating metal components as large as 12x12x10 in. Typical process speed is 10-20 in<sup>3</sup>/hr, depending on resolution. Components were thermally processed in a non-vacuum atmosphere furnace. Metal powders and binder were used as obtained from commercial vendor (Extrude Hone Corporation, Irwin, PA). Experimental strain measurements were measured pre- and post-sintering using a Smart Scope non-contact video measuring device (Optical Gaging Products, Inc.). The Smart Scope measuring method selects several points along each edge of the sample at a magnification of 53x. A least squares linear fit is used for the edges of the samples. Dimensional measurements are calculated from the linear fit lines with an accuracy of  $\pm 40\mu\text{m}$  (0.00015 in.). Experimental results for 3DP™ samples printed using 20-, 80-, and 200- $\mu\text{m}$ -diameter diameter spherical powder particles are shown in Table 3.

The analytical calculation of the strain requires that the material properties of the sintering media, namely 316L SS, be known. Material properties for 316L SS used for the analytical calculations are presented in Table 4. The magnitudes of the analytically calculated strain are shown in Table 4 where the values can be readily compared to the measured values for 20, 80, and 200  $\mu\text{m}$  diameter particles. The calculated analytical strain is approximately one order of magnitude less than the experimentally obtained strain measurements. A graphical representation of the analytical strain development for a defined sintering temperature profile is presented in Figure 5.

**Table 3.** Comparison of experimental measured and calculated strains for X-print direction, ( $\mu\text{m}/\mu\text{m}$ ).

| Powder Particle Diameter ( $\mu\text{m}$ ) | Experimental Strain Measurements | Calculated Analytical Strain |
|--|----------------------------------|------------------------------|
| 20   | 0.1314                           | 0.012850                     |
| 80   | 0.0166                           | 0.002860                     |
| 200  | 0.0098                           | 0.000812                     |

**Table 4.** Material properties of 316L SS powder particles.

|                                     |
|-------------------------------------|
| $Q_v = 280 \text{ kJ/mol}$          |
| $\gamma = 2 \text{ J/m}^2$          |
| $\Omega = 6.9565 \text{ mol/cm}^3$  |
| $D_v = 40,000 \text{ m}^2/\text{s}$ |

The strain curve shown in Figure 5 is indicative of the intuitive progression of neck growth and strain. Comparing the temperature profile and the corresponding analytically computed strain, it is observed that strain does not readily increase until the temperature reaches approximately 825 °C, which conforms with [6]. It should also be noted that after the sintering temperature has been reached and the samples begin to decrease in temperature, sintering activity becomes negligible, which corresponds to no additional strain (neck growth).

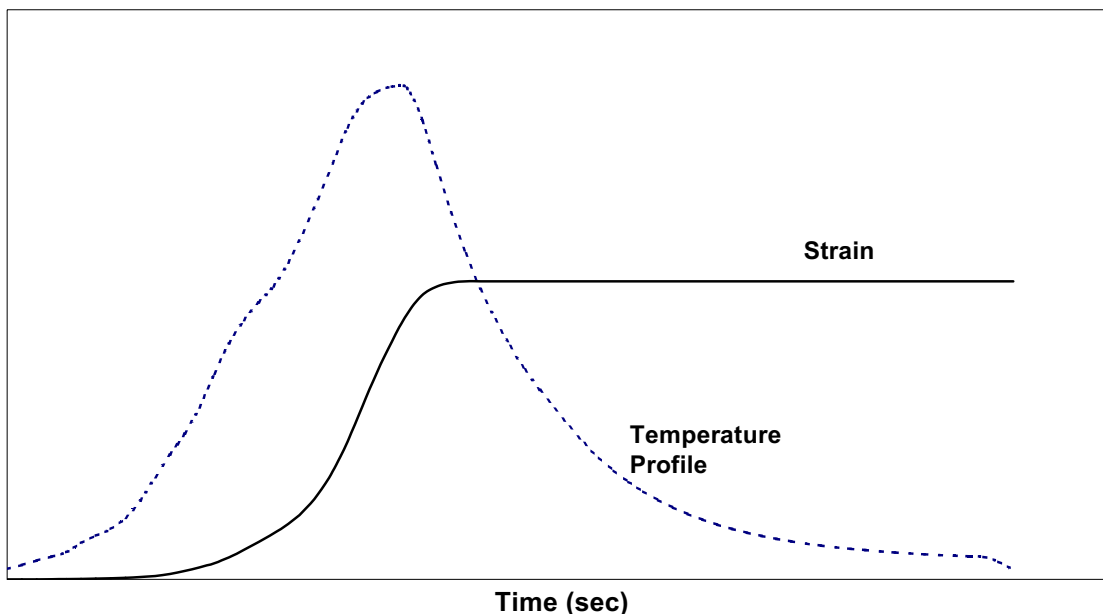


**Figure 5.** Typical sintering temperature profile displayed with the corresponding strain calculated using the strain rate surface.

It has been noted by German [1,2], that the equations describing initial stage sintering are only approximations and should be considered as such. The authors propose that a modification of these equations will lead to relatively accurate prediction of sintering strains which can be applied to the 3DP™ sintering processes. All of the contributing factors of Equations 1 and 2 have accepted values except for powder particle diameter,  $D$ . The only option for any type of modification to Equation 1 would be to alter the particle diameter influence.

### Effective Particle Size, $D_{eff}$ , Formulation

The discrepancy between the analytical formulation and experimental results can be accounted for by creating an effective particle size parameter to use in the analytical formulation. To formulate the new parameter, experimental study involving sintering strains produced within components comprised of particles with different diameters was performed. Since 3DP™ predominantly creates components using particle diameters in the range of 20-100  $\mu m$ , experimentation was performed using samples that were comprised of 20-, 80-, and 200- $\mu m$  spherical powder to allow for a range of experimental values to be obtained. It should be noted that the powder particle diameter is not constant throughout the component; however the particle diameters are highly concentrated about their respective mean diameter (20, 80, and 200  $\mu m$ ).

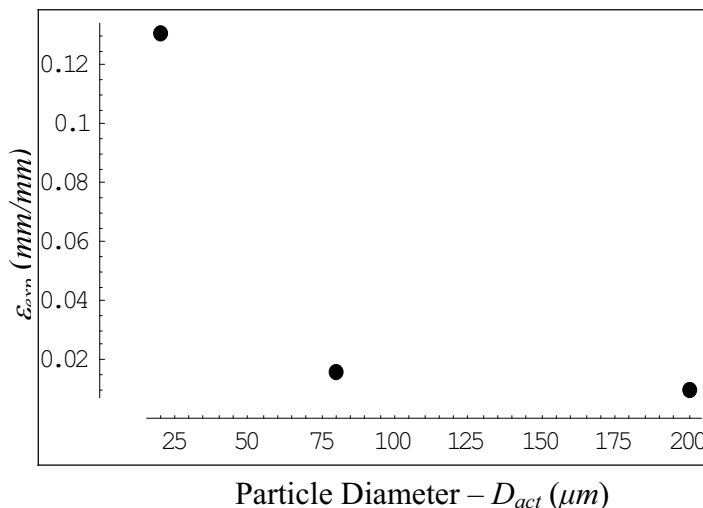


**Figure 6.** Powder particle diameter compared to experimentally measured sintering strain.

Table 3 indicates that the magnitude of the strain calculated using the strain rate surface has values less than the experimentally measured strain. It is also observed in Equation 1 that the strain does not possess a simple linear relationship with particle diameter. Figure 6 displays a graphical representation of the data displayed in Table 3; note the non-linear relationship between the strain and the powder particle diameter. Therefore, a constant correction factor will not suffice as an effective particle diameter. The strain increases as the particle size decreases, which is consistent with the algebraic relation of strain and particle diameter defined in Equation 1.

It is proposed to introduce an effective particle diameter to use in the analytical calculation as a parameter indicative to 3DP™ sintering. The effective particle diameter is determined by calculating what effective particle diameter is required to produce the experimentally measured strain, while using the strain rate analysis calculation method. The effective diameter,  $D_{eff}$ , would then be dependant upon the sintering temperature profile that was used during the experimental work as well as the actual diameter of the powder particles,  $D_{act}$ , namely:

$$D_{eff} \equiv D_{eff}(D_{act}, t, T) \quad (5)$$

The sintering temperature profile must be accounted for while formulating the analytical form of  $D_{eff}(D_{act}, t, T)$ . Examination of Equation 1 (for VD) reveals that the isothermal strain curve,  $\varepsilon \equiv \varepsilon(t)$ , can be thought of as:

$$\varepsilon \equiv \varepsilon(t, T, D) = \left( \frac{B \cdot t}{2^5 D^3} \right)^{2/5} \quad (6)$$

Using Equation 6, a fixed time,  $t$ , and fixed temperature,  $T$  (isothermal temperature profile), and with the experimentally obtained strain values, it is possible to solve for an effective particle diameter,  $D_{eff}$ , for each of the 20-, 80-, and 200- $\mu\text{m}$  samples. The effective diameter,  $D_{eff}$ , would then be dependant upon the chosen isothermal temperature profile.

The only known values for actual strain production are obtained from the experimental temperature profile,  $T_{exp}(t)$ . To find the effective particle diameters for  $T_{exp}$ , successive strain rate analyses were performed to obtain a relationship between the particle diameter and produced strain. Next the strain values were back-solved to find the effective particle diameter for  $T_{exp}$ . Those results are shown in Figure 7. The relationship of the effective particle diameter,  $D_{eff}$ , to the actual diameter,  $D_{act}$ , can be defined by a logarithmic relationship, and the effective data points were fitted to the generic equation:

$$D_{eff}(D_{act}) = A \cdot [\ln(D_{act}) + B] \quad (7)$$

resulting in

$$D_{eff}(D_{act}) = 11.0 \cdot [\ln(D_{act}) - 2.7]. \quad (7')$$

Again, it should be noted that Equation 7' represents a  $D_{eff}$ , which is dependant upon  $T_{exp}$ .

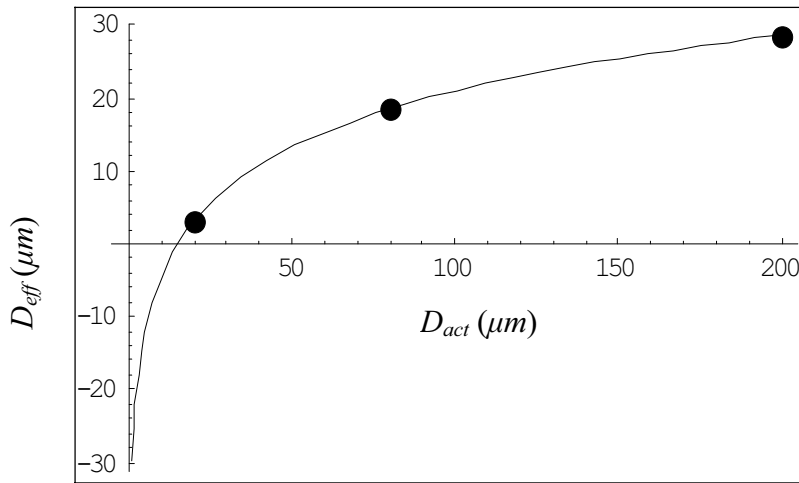


**Figure 7.** Actual particle diameter compared to the effective particle diameter.

The fitted curve for  $D_{eff}$  represented by Equation 7' can be expanded to be used for any temperature profile. Introduction of a temperature profile factor ( $TPF$ ) whose value will be dependent upon the active sintering area of the temperature profile. The active sintering area for a material can be defined as the time where the temperature exceeds a threshold temperature where strain begins to form. Strain begins to form before the sintering temperature is reached, which is observed in Figure 5 and for 316L SS, temperatures above 825 °C (or 1100K) are the most active temperatures for sintering [3,6]. For sintering of 316L SS, it is possible to relate the active area for any sintering profile to  $T_{exp}$ , creating a  $D_{eff}$  for that particular profile. Therefore Equation 7' can be modified such that:

$$D_{eff}(D_{act}) = TPF \cdot 11.0 \cdot [\ln(D_{act}) - 2.7] \quad (8)$$

where  $TPF$  is the sintering temperature profile factor.

A possible definition of the  $TPF$  is defined as the ratio of the integral of  $T_{exp}$ , to the integral of  $T_{profile}$ , where their respective temperatures exceed 1100K, namely:

$$TPF = \frac{\int_{T \geq 1100} T_{exp}(t) dt}{\int_{T \geq 1100} T_{profile}(t) dt} \quad (9)$$

Equation 9 displays an intuitive relationship between any  $T_{profile}$  when compared to results for  $T_{exp}$ . The longer a component is exposed to temperatures within its active sintering area, the more strain is produced. This relationship between the temperature profile and the effective particle diameter,  $D_{eff}$ , creates an initial foundation from which to produce quantitative results for sintering of 316L SS 3DP™ components.

## Conclusions

This study expands upon the qualitative initial stage isothermal sintering strain equations presented by German [2] by creating a strain rate surface. Using the strain rate surface, it is possible to analyze and qualitatively predict dimensional change of initial stage sintering

subjected to any sintering temperature profile by solving the corresponding ODE. The result is a time strain relation for the applied temperature profile

Comparing experimentally obtained strain values and analytically calculated strain values using different diameter particles demonstrates the influence of powder particle diameter upon sintering strain in 3DP™ components. The experimental results are consistent with the theory that powder particle diameter is a dominating influence upon initial stage sintering strain. The relationship between the powder particle diameter and corresponding sintering strain introduces a method to create quantitative results for sintering analysis of 3DP™ components in the form of an effective particle diameter.

The strain rate surface, when combined with experimental strain measurements, provides an analytical form for an effective particle diameter. The effective particle diameter has been formulated such that it is dependant upon the corresponding sintering temperature profile to be applied. Using the effective particle diameter within the analytical strain calculation (strain rate surface) yields quantitative results of sintering strain for 316L SS 3DP™ components.

### **Future Endeavors**

Additional experimentation is required to formulate a rigorous relationship between the *TPF* and the experimental temperature profile. Several sintering runs must be performed using temperature profiles that possess drastically different sintering activity areas. This experimental study would allow for a more concrete definition of the *TPF*.

The analytical method developed herein can be expanded upon by incorporating dimensional strain computations into a Finite Element Analysis. Including isotropic strain formulation characterized by Johnston [8], a three-dimensional strain analysis can be performed for 3DP™ components. By combining strength values and fracture or failure modes, it becomes possible to predict problematic sintering profiles for component geometry.

Further development of this theory is possible to include components that are comprised of powder particles of different diameters, thereby creating components with increased green and sintered densities.

### **Acknowledgements**

Financial support for this work is provided by the Office of Naval Research, Contract #N00014-C-00-0378. The authors are grateful to the Physics Department at University of Washington for equipment use.

### **References**

- [1] R. German, *Computer Modeling of Sintering Processes*, The International Journal of Powder Metallurgy, Vol. 38, No. 2, 2002, p. 48-66.
- [2] R. M. German, *Sintering Theory and Practice*, Wiley & Sons, New York, 1996.

[3] ASM International, *Powder Metal Technologies and Applications*, ASM Handbook, Volume 7, 1998, pp.448-452.

[4] E. Sachs, P. Williams, M. Brancazio, Cima, and K. Kremmin, *Three Dimensional Printing: Rapid Tooling and Prototypes Directly From a CAD Model*, Proceedings of Manufacturing International, ASME, 4, 1990, pp. 131-136.

[5] F. Thümmler and R. Oberacker, *An Introduction to Powder Metallurgy*, The University Press, Cambridge, 1993.

[6] R. German, *Powder Metallurgy Science*, 2<sup>nd</sup> ed., Metal Powder Industries Federation, Princeton, NJ, Chapters 7 and 9, 1997.

[7] *Mathematica* 4.2, A product of Wolfram Research, Inc.

[8] S. Johnston and R. Anderson, *Finite Thermal Analysis of Three Dimensionally (3DP™) Printed Metal Matrix Composites*, Proceedings of the 13<sup>th</sup> Annual Solid Freeform Fabrication Symposium, Austin, TX, August 2002.